

NEUTRONIC DESIGN OF A FLUIDIZED BED REACTOR

J.L. Kloosterman
H. van Dam
V.V. Golovko
T.H.J.J. van der Hagen
Delft University of Technology
Interfaculty Reactor Institute (IRI)
Mekelweg 15
NL-2629 JB Delft, Netherlands
E-mail: J.L.Kloosterman@iri.tudelft.nl

R.F. Mudde
Delft University of Technology,
Kramers Laboratorium voor Fysische
Technologie
Prins Bernardlaan 6, NL-2628 BW Delft,
Netherlands

ABSTRACT

FLUBER is a conceptual design of a fluidized bed reactor, which consists of TRISO coated fuel particles with outer diameter of 1 mm contained in a graphite-walled cavity. When the helium coolant starts to flow in upward direction, the particle bed gets fluidized and reactivity increases due to the influence of the reflector. The maximum reactivity that can be introduced this way is limited, because the reactor becomes subcritical again due to increased neutron leakage when the particle bed expands further. As a result, the reactor is critical only for a specific range of coolant flow rate, which limits inherently the maximum power that can be generated.

The reactivity coefficients of temperature are calculated for the fuel, moderator and reflector zones. The first two are negative, the last one positive, but the overall effect is negative. The contributions to the temperature coefficients are calculated for each factor of the four-factor formula, showing that the Doppler effect dominates the temperature coefficient of the fuel, and that spectral shift effects dominate the temperature coefficient of the moderator.

Experiments have shown that the particle flow in the core region is highly turbulent. The influence of three fuel particle density distributions on reactivity is investigated. Although different, all distributions show the same trends.

I. INTRODUCTION

This article describes the neutronic design and reactivity coefficients of a fluidized bed reactor fuelled with small particles and cooled with helium. This Fluidized Bed Reactor (FLUBER) [1] has a potential for

inherently safe and economic operation due to its reactivity feedback characteristics, high specific power, flexible on-line refueling, and high thermal efficiency.

FLUBER consists of a graphite cylinder with diameter of about 3 m and height of 8 m. Inside the cylinder, a core cavity with cross section of 1 m² and height of 6 m is partly filled with small TRISO coated fuel particles [2]. The dimensions of the core and reflector are given in Table 1.

Table 1. Specification of FLUBER.

Radius of core cavity [cm]	56.4
Height of core cavity [cm]	600
Height of whole reactor [cm]	800
Thickness of radial reflector [cm]	100
Thickness of axial reflectors [cm]	100
Collapsed-bed height [cm]	136
Density reflector material [g cm ⁻³] (nuclear graphite)	1.763
Uranium fuel inventory [kg]	120
Fuel enrichment (wt%)	16.76
Helium coolant density* [g cm ⁻³]	2.42·10 ⁻³

* The coolant density corresponds with a pressure of 50 bar and a temperature of 1000 K

Each TRISO particle consists of a spherical kernel containing low enriched uranium dioxide covered with a concentric porous carbon buffer layer, a pyrolytic carbon layer, a silicon carbide layer, and again a pyrolytic carbon layer. The pyrolytic and silicon carbide layers prevent the release of fission products from the fuel particles even in case the core cooling fails. The silicon carbide layer also improves the mechanical strength to withstand external forces. Although the design of the fuel particles is not yet finalized, the

composition used for the calculations presented here is given in Table 2.

Table 2. Fuel composition of TRISO particle [3].

Material	Density [g cm ⁻³]	Outer diameter [mm]
UO ₂ kernel	10.88	0.26
Porous carbon buffer layer	1.1	0.77
PyC coating	1.9	0.85
SiC coating	3.2	0.92
PyC coating	1.9	1.00

Helium, which flows from bottom to top through the core cavity, is used both as a coolant and to fluidize the particle bed. In collapsed state, the core is strongly subcritical. When the helium flow increases, the particle bed expands and neutrons leak away from the core to the graphite, where they are moderated and reflected. Effectively, this increases the moderator-to-fuel ratio of the system, which makes the reactor critical. However, for a helium flow too large, too many neutrons leak away and the system becomes subcritical again. As a consequence, with a proper choice of system parameters, the reactor is critical only for a limited range of coolant flows.

After describing the calculation procedures in section II of this article, we show the results of the fuel and moderator temperature reactivity coefficients in section III. The behavior of reactivity as a function of the particle bed expansion height is shown in section IV, and the behavior of reactivity for different fuel particle distributions in section V.

II. CALCULATIONAL PROCEDURES

All calculations have been carried out by the INAS code system (IRI-NJOY-AMPX-SCALE) with nuclear data libraries based on the JEF2.2 data file.

The major part of the calculations for the temperature reactivity coefficients is done with the CSAS driver of the SCALE system [4]. The CSAS module calculates resonance-shielded cross sections by use of the Bondarenko method in the unresolved region and the Nordheim method in the resolved region. The result is a zone-weighted multi-group library in AMPX format, which can be used by the one-dimensional XSDRNPM-S discrete-ordinates program or by the three-dimensional KENO-VA Monte Carlo program. Furthermore, the library can be converted to ISOTX format used by BOLD-VENTURE [5] or to the multi-group format used by MCNP [6].

For the resonance shielding calculations, Dancoff factors are needed to account for the probability that a neutron that leaves a fuel kernel enters another kernel without a collision in between. These factors are

calculated by the DANCOFF-MC computer program [7] based on the Monte Carlo method.

The fast fission factor, the resonance escape probability, the thermal utilization and the average number of neutrons released per thermal absorption in the fuel (the four-factor formula) were calculated by VAREX [8]. This program uses the AMPX working libraries and the output and flux files of forward and adjoint XSDRNPM-S runs.

The k_{eff} for R-Z geometry (2-D) was calculated by the diffusion code BOLD-VENTURE and by the Monte Carlo codes MCNP4B and KENO-VA [4].

III. TEMPERATURE COEFFICIENTS OF REACTIVITY

The fuel and moderator temperature coefficients of reactivity are important parameters for the evaluation of transients in FLUBER. For a safe operation, both coefficients should be negative for the whole range of expanded core heights. This range is simulated by one-dimensional calculations on a fuel particle with a variable fuel kernel diameter and a fixed particle outer diameter (1 mm). The CSAS module was used to calculate the k_{eff} as a function of the moderator-to-fuel ratio, and the VAREX program to calculate the individual contributions to the temperature coefficients.

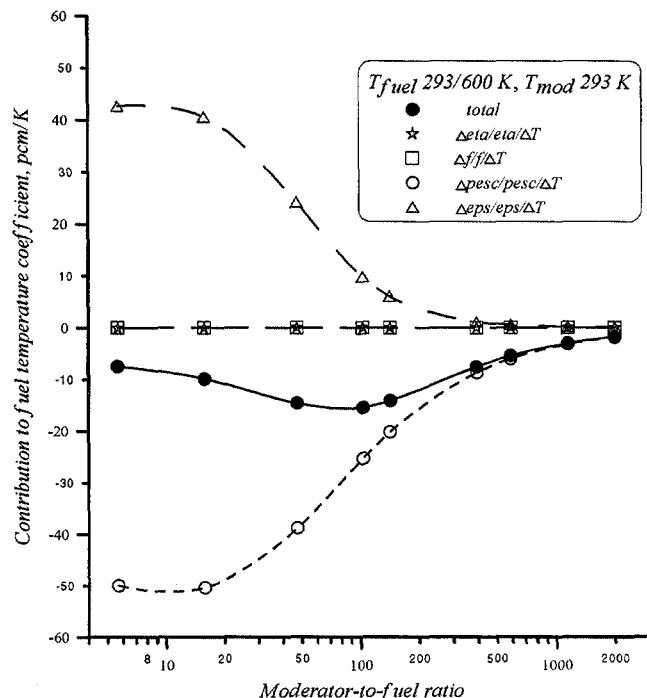


Figure 1. Components of the fuel temperature coefficient as a function of the moderator-to-fuel ratio. The k_{∞} values were calculated for fuel temperatures of 293 and 600 K with constant moderator temperature of 293 K. The effects due to ϵ and p dominate.

For each value of the moderator-to-fuel ratio, the Dancoff factor was calculated by DANCOFF-MC.

When the effective multiplication factor k_{eff} is used to calculate the temperature coefficient, the correct formula would be:

$$\alpha = \frac{1}{k_{hot} k_{cold}} \frac{k_{hot} - k_{cold}}{\Delta T} \quad (1)$$

where ΔT is the temperature difference of either the fuel or moderator. However, in our case we used the infinite multiplication factor k_{∞} to calculate the temperature coefficients, and the appropriate formula to calculate this reads [9]:

$$\alpha^* = \frac{2}{k_{hot} + k_{cold}} \frac{k_{hot} - k_{cold}}{\Delta T} \quad (2)$$

Using the four-factor formula, k_{∞} can be written as $k_{\infty} = \epsilon p f \eta$, where ϵ is the fast fission factor (including epithermal fissions), p the resonance escape probability, f the thermal utilization factor, and η the number of neutrons released per thermal absorption in the fuel. In terms of the four-factor formula the temperature reactivity coefficient becomes:

$$\alpha^* = \frac{1}{\eta} \frac{\partial \eta}{\partial T} + \frac{1}{f} \frac{\partial f}{\partial T} + \frac{1}{\epsilon} \frac{\partial \epsilon}{\partial T} + \frac{1}{p} \frac{\partial p}{\partial T} \quad (3)$$

All four contributions to the temperature reactivity coefficients have been calculated as a function of the moderator-to-fuel ratio. Figure 1 shows the results for the fuel temperature coefficient, where the fuel temperature has been increased from 293 K to 600 K. The changes in η and f on the RHS of Eq. 3 give virtually zero contribution, while the changes in ϵ and p give large contributions with opposite sign. Increasing the fuel temperature increases the resonance absorption, which increases the fast fission factor and reduces the resonance escape probability. The net effect is strongly negative (between -10 and -20 pcm K^{-1}) shown by the filled dotted line. For large moderator-to-fuel ratios, the effects decrease due to the softening of the neutron spectrum.

The mechanism responsible for the positive reactivity feedback due to the fast fission factor ϵ can be explained by looking at the definition of ϵ :

$$\epsilon = \frac{t + n}{t}, \quad (4)$$

where t is the neutron production rate by thermal fissions and n is the production rate by non-thermal fissions. The fast fission factor depends on temperature as:

$$\frac{\partial \epsilon}{\partial T_F} = \frac{\partial}{\partial T_F} \left(\frac{n}{t} \right) = \frac{\partial n}{\partial T_F} \frac{1}{t} - \frac{\partial t}{\partial T_F} \frac{n}{t^2} > 0 \quad (5)$$

When the fuel temperature rises, two effects occur: fission resonances broaden and the Maxwell thermal spectrum shifts to higher energies. This implies that the first derivative on the RHS of Eq. 5 is positive, while the second is negative. The difference of these two terms always gives a positive reactivity feedback.

On the other hand, Doppler broadening of the fission and capture resonances after a fuel temperature increase gives a decrease of the resonance escape probability p , which gives a negative reactivity feedback.

In figure 2, results are given for the moderator temperature coefficient. The k_{∞} values were calculated for moderator temperatures of 293 to 600 K with a constant fuel temperature of 293 K. In this case, the influence of the temperature on ϵ and p is very small, while it has large effects on f and (to a lesser extent) on η . The thermal utilization reads:

$$f = \frac{1}{1 + \zeta \frac{\sum_{aM} V_M}{\sum_{aF} V_F}} \quad (6)$$

where \sum_{aM} and \sum_{aF} are the macroscopic absorption cross sections of the moderator and fuel, respectively, and ζ is the thermal disadvantage factor ($\zeta \equiv \phi_{thM} / \phi_{thF}$).

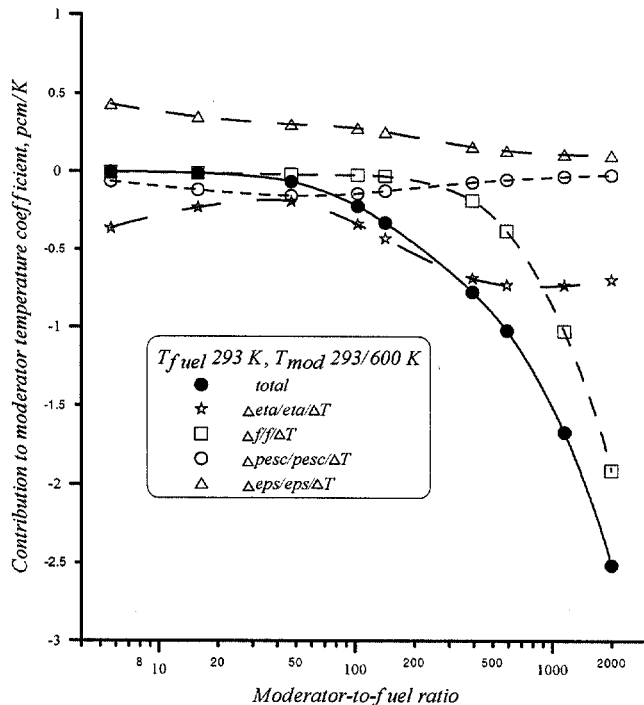


Figure 2. Components of the moderator temperature coefficient as a function of the moderator-to-fuel ratio. The k_{∞} values were calculated for moderator temperatures of 293 and 600 K with constant fuel temperature of 293 K. The effects due to η and f dominate.

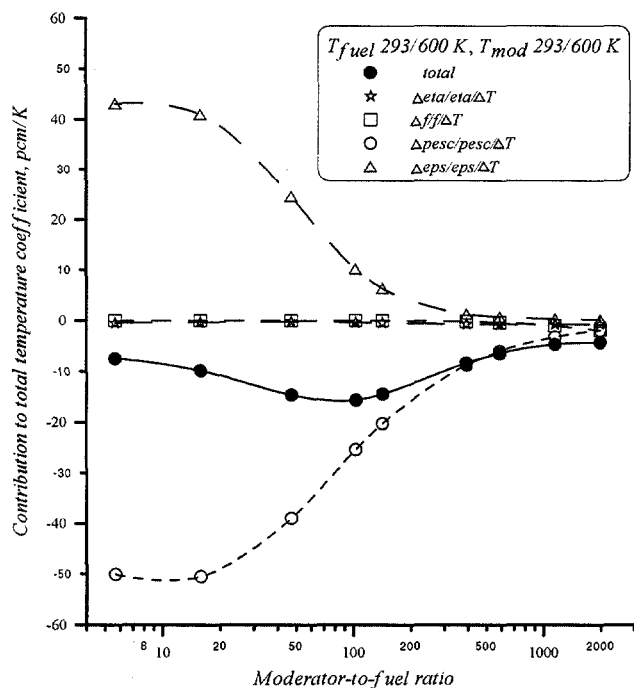


Figure 3. Components of the uniform temperature coefficient as a function of the moderator-to-fuel ratio. The k_{∞} values were calculated for fuel and moderator temperatures of 293 and 600 K. The effects due to ϵ and ρ dominate.

Increasing the moderator temperature shifts the thermal neutron spectrum to higher energies, which reduces both the ratio of macroscopic absorption cross sections and ζ . The first because the U-235 absorption cross sections falls off faster than the graphite $1/\nu$ cross section, the second term because the thermal flux depression in the fuel decreases. This means that the reactivity effect of f is always negative.

For our case, η can be found from the formula:

$$\eta = \frac{\nu}{\frac{\Sigma_{aU35} + \Sigma_{aU38}}{\Sigma_{fU35}} + \frac{\Sigma_{aU38}}{\Sigma_{fU35}}}, \quad (7)$$

where ν is the average number of neutrons released per fission, Σ_f is the macroscopic fission cross section and Σ_a the macroscopic absorption cross section. The first factor in the denominator of Eq. 7 is almost independent of temperature, while the second factor increases because the U-238 cross section has a $1/\nu$ dependence, while the U-235 cross sections falls off faster with energy.

Figure 3 shows the uniform temperature coefficient of reactivity as a function of the moderator-to-fuel ratio. Because the fuel temperature coefficient is much larger than the moderator temperature coefficient, figure 3 is very similar to figure 1. This means that the Doppler

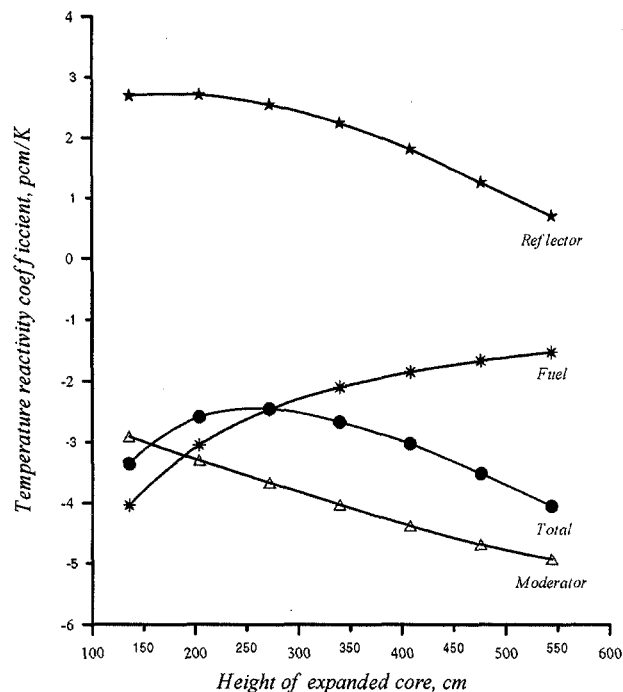


Figure 4. Uniform temperature coefficient of reactivity as a function of expanded core height, assuming a uniform distribution of fuel particle in the core cavity. These are results from the two-dimensional model calculations with BOLD-VENTURE.

coefficient dominates the temperature reactivity feedback.

To calculate the temperature coefficients of reactivity for the whole core, a two-dimensional model of the core region and axial and radial reflector zones was made and calculations were done with the BOLD-VENTURE code. This model is described in more detail in the next section, but the results on the temperature coefficients are reported here to complete this section.

Figure 4 shows the temperature coefficient as a function of expanded core height, assuming a uniform distribution of fuel particles in the core region. Because k_{eff} is calculated instead of k_{∞} , Eq. 1 is used to calculate the reactivity coefficients and not Eq. 2, which was applied to calculate all previous results. Clearly, the temperature reactivity coefficient is negative for all expanded core heights. It is smallest negative for a core height of about 270 cm.

Also the contributions of the fuel, moderator and reflector are shown in figure 4. The calculations of k_{eff} have been done for two different temperatures, 293 K and 1243 K, corresponding with room temperature (20 °C) and hot full power (950 °C). To calculate the contribution of a specific zone (fuel, moderator or reflector), only the temperature of that zone was increased.

As expected from figures 1 and 2, the fuel and moderator temperature coefficients are negative for the whole range of expanded core heights. The fuel temperature coefficient is strongest negative in case of a fully collapsed bed (height of 136 cm). Because the particles have an outer diameter of 1 mm and a fuel kernel diameter of 0.26 mm, the moderator-to-fuel atomic ratio equals 160. In figure 1, the fuel temperature coefficient for moderator-to-fuel ratios larger than 160 decreases with increasing ratio, which corresponds with an increase of the expanded core height in figure 4.

The contribution due to the moderator temperature coefficient is negative, because a shift of the thermal Maxwell spectrum to higher energies favors absorption by U-238 relative to absorption by U-235. It is strongest negative for a fully expanded bed.

The contribution due to the reflector temperature coefficient is positive, and largest for a collapsed bed. In general, increasing the reflector temperature decreases the absorption rate by the graphite and increases the number of reflected neutrons, which leads to an increase of reactivity.

IV. TWO DIMENSIONAL MODEL

Due to the influence of the reflector on reactivity, k_{eff} is a complex function of expanded core height, which cannot be accurately calculated in a one-dimensional model. Therefore, a two-dimensional geometry of the reactor was modeled in both BOLD-VENTURE, KENO-VA, and MCNP4B (in multi-group mode). To be sure these codes give coherent results, they were first compared with each other for a simple one-dimensional geometry containing an infinitely long particle bed surrounded by a graphite cylinder with thickness of 1 meter. To simulate core expansion, two different densities for the particle bed were used, one corresponding with a fully collapsed particle bed (corresponding with a core height of 136 cm), and one with a four-times expanded particle bed (core height of 544 cm). All codes used the same 172-group cross section library. Results for k_{∞} are given in Table 3, which shows that all results are in good agreement with each other within 0.2%.

Table 3. Multiplication factor for infinite cylinder.

Codes	k_{∞} (136 cm)	k_{∞} (544 cm)
XSDRNPM	1.1638	1.0500
BOLD-VEN	1.1629	1.0492
KENO-VA	1.1638 \pm 0.0007	1.0479 \pm 0.0008
MCNP4B	1.1636 \pm 0.0007	1.0485 \pm 0.0009

As mentioned before, reactivity of the core is a function of expanded core height. BOLD-VENTURE,

KENO-VA and MCNP4B were used to calculate the reactivity as a function of expanded core height with a uniform particle density. For the latter two codes, a 172-group cross-section library was used, while for BOLD-VENTURE a 49-group cross-section library was used derived from the 172-group library. The results given in figure 5 show that reactivity increases up to a core height of about 270 cm. When the core expansion continues, reactivity decreases again. Apparently, when the core height increases from 136 to 270 cm, neutrons that leak away from the core are effectively moderated and reflected. However, for heights larger than 270 cm, too many neutrons leak away and too many are absorbed in the reflector. As a result, k_{eff} decreases.

The BOLD-VENTURE results deviate from the Monte-Carlo ones, which is probably due to inappropriate treatment by diffusion theory of the vacuum between the top of the core and the upper reflector. Although the reactivity curve obtained with BOLD-VENTURE is similar to those of the Monte-Carlo codes, the top of the curve is at a lower k_{eff} value (1.003), while for a fully expanded core k_{eff} is larger (0.994). These differences may be of importance to assess the dynamic behaviour of the reactor. It has been verified that using in BOLD-VENTURE the 172-group data library that was also used for the Monte-Carlo calculations does not give a large improvement.

To investigate the effects of group-wise cross-section data libraries, two calculations were done with MCNP-4B using a point-wise cross-section data library based on ENDF/B-VI. The calculations were done for core heights of 136 cm (fully collapsed bed), 272 cm

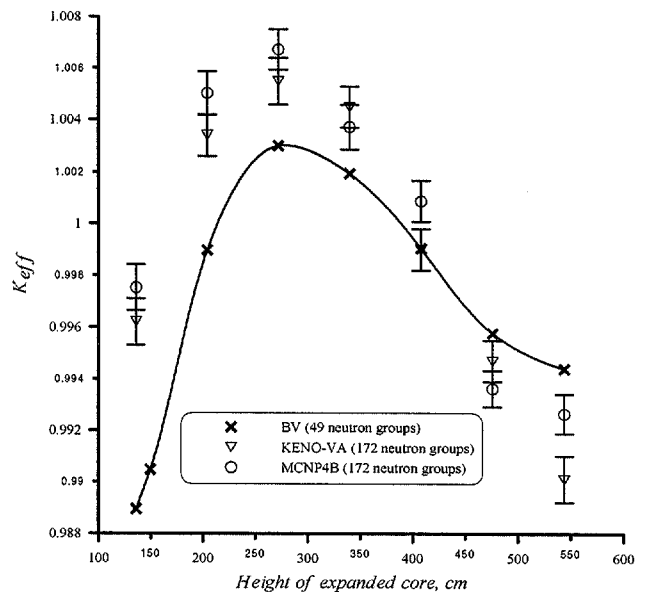


Figure 5. The k_{eff} as a function of expanded core height calculated by diffusion code (BV) and group-wise Monte Carlo (KENO-VA and MCNP-4B). The nuclear data libraries are based on JEF2.2.

and 544 cm. The results agreed within 0.3% with the group-wise MCNP values shown in figure 5.

V. EXPERIMENTAL RESULTS

Until now, all results were calculated for a uniform distribution of fuel particles in the core region. However, experiments show that the particle density is inhomogeneous, and that a linearly decreasing particle density from bottom to top would be more appropriate. This section describes the experimental results that give an indication of the particle distribution in the cavity.

Particle flow through the core is highly turbulent. Experiments with an air-fluidized bed with collapsed bed height of 51 cm and cavity diameter of 38.4 cm show that particles are transported in upward direction through the whole cross section of the bed, but that

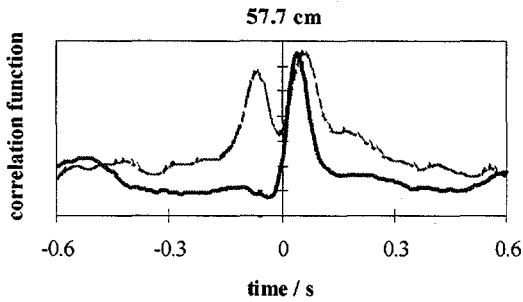


Figure 6. Correlation function of the signals of two axially displaced sensors measuring gamma transmission through the center of the core (solid line) and through the periphery (dashed line). A peak at positive times indicates upward transport of particles, a peak at negative time downward transport.

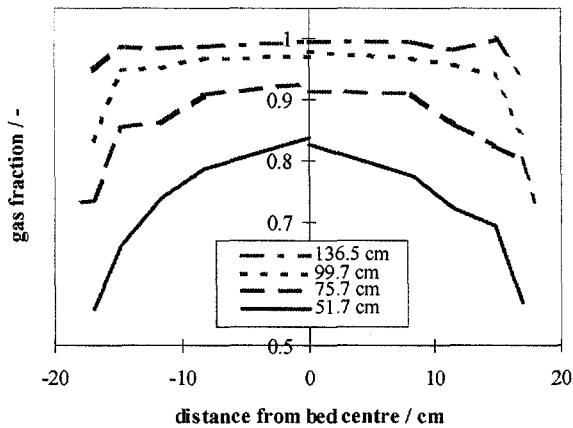


Figure 7. Radial gas-fraction profiles measured at several heights in the experimental fluidized bed. Collapsed bed corresponds with a height of 51 cm.

downward transport mainly occurs along the periphery. Figure 6 shows the results of gamma transmission experiments [10] of two axially displaced gamma sensors. It is seen that particles move in upward direction along the centerline of the core, while they move in upward and downward direction along the periphery.

Besides this, the particle density is not static: clusters of particles and bubbles of helium move chaotically through the core in an alternating way. This gives a complex space- and time dependent behavior of the particle density in the core. Figure 7 shows the radial gas-fraction profile at several heights of the expanded particle bed. Clearly, the gas fraction increases with expanded bed height, which can have a significant impact on reactivity. This is investigated in the next section.

VI. PARTICLE DENSITY DISTRIBUTIONS

To study the impact of different particle density distributions on reactivity, three cases were considered:

1. Uniform distribution of fuel particles in the core.
2. Linearly decreasing particle density in the core (from collapsed-bed density at the bottom to zero density at the top).
3. Uniform distribution of 85% of the fuel particles in the lower part of the active core, and a linearly decreasing density of the remaining 15% of the fuel particle in the upper

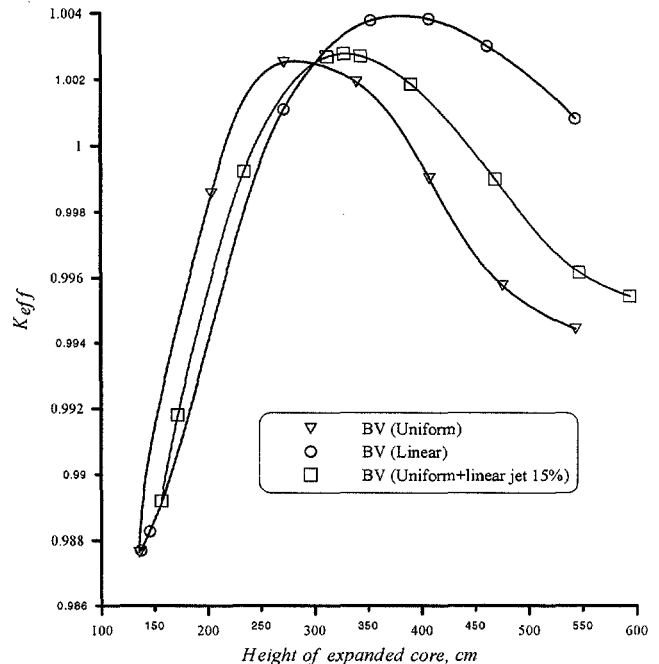


Figure 8. The k_{eff} as a function of fluidized core height for three particle distributions, as calculated by BOLD-VENTURE.

part of the active core. This simulates 'jets' of fuel particles emitted from the core into the cavity above.

Figure 8 shows k_{eff} as a function of the expanded core height calculated by BOLD-VENTURE. The shape of the curves is very similar for the uniform distribution (case 1) and the uniform distribution with linear jets above the core region (case 3). In figure 8, the latter curve is somewhat shifted to the right (towards larger expansion heights), which reflects the fact that for case 3 the height of the active core is always larger, because 15% of the active core has a linearly decreasing particle density instead of a uniform one. Because the adjoint function in this part of the core is low compared to the adjoint function at the bottom of the core, the particle distribution in the upper part of the active core has not a large influence on reactivity.

A larger difference exists between the uniform distribution (case 1) and the linearly decreasing one (case 2). For the latter, the maximum k_{eff} is larger, while the difference between the maximum value and the k_{eff} at maximum core expansion (at about 600 cm) is much smaller than for the uniform distribution.

For both distributions, uniform and linearly decreasing, the thermal flux peaks in the bottom reflector, but for the linear distribution, this effect is much stronger due to the higher particle density at the bottom of the core. For expanded core heights between a factor of two and four times the collapsed core height, the particle density at the bottom for the linearly decreasing distribution is two times that of the uniform

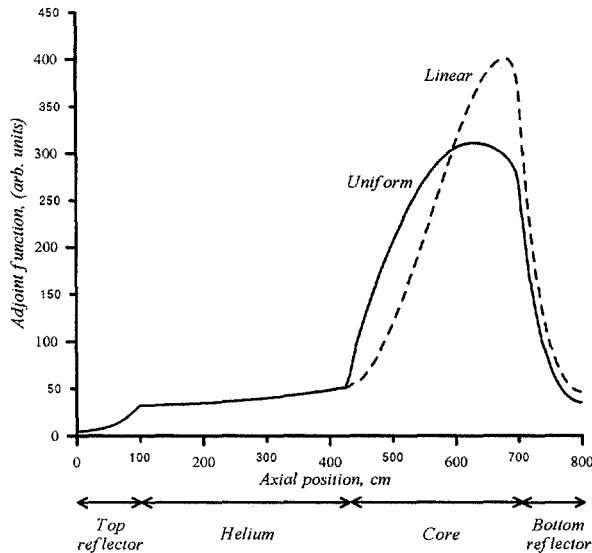


Figure 9. The adjoint function as a function of axial position. The solid line corresponds with a uniform distribution of fuel particles, the dashed line with a linearly decreasing distribution. The expanded core height equals 272 cm.

distribution. Due to the influence of the bottom reflector, the adjoint function peaks close to the bottom reflector. In effect, the linear distribution is more reactive than the uniform distribution with equal fuel inventory.

The adjoint function for both distributions is shown in figure 9 as a function of the axial position. In this figure, the origin of the X-axis corresponds with the top of the reactor (outer side of top reflector), and position 800 cm with the outer side of the bottom reflector. The positions between 100 and 700 cm correspond with the core cavity (100 cm is the top, 700 cm the bottom). The expanded core height equals 272 cm, which implies that the active core zone ranges from 700 (bottom) to 432 cm. Clearly, the adjoint function peaks in the lower part of the active core zone. For the linear distribution, the peak is higher and closer to the bottom reflector.

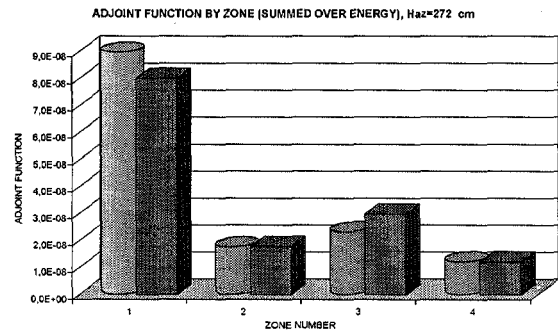


Figure 10. Adjoint function per zone (summed over energy). Calculations were performed with BOLD-VENTURE assuming a uniform particle density distribution (cylindric shape) and a linearly decreasing density (cubic shape).

Figure 10 shows the adjoint function per zone for two different particle distributions. Both calculations are done for a fluidized core height of 272 cm. Zone 1 corresponds with the active core, zone 2 with the cavity between the active core and the top reflector, zone 3 with the top and bottom reflectors, and zone 4 with the radial reflector. Due to the relative large particle density close to the bottom reflector, the adjoint function for the axial reflectors (zone 3) is higher for the linearly decreasing particle density, while for the uniform distribution the adjoint function is higher for the core zone.

VII. DISCUSSION AND CONCLUSIONS

The neutronic properties of a conceptual fluidised bed reactor have been calculated. Although the design is not yet final and optimisation is still possible, several interesting features can be seen.

First, with the current fuel particle design, the reactivity coefficient of temperature is negative due to

the Doppler effect and, to a lesser extent, due to spectral shift effects in the thermal energy range. The reactivity coefficient of the graphite reflector is positive due to spectral shift effects, but this is compensated by the large negative value of the fuel and moderator zones. It is not likely that the combined effect will give a positive reactivity introduction, as this would require a temperature increase of the reflector much larger than that of the fuel and moderator. Furthermore, heating of fuel and moderator is almost a prompt effect, while the heating of the reflector is much more delayed.

Secondly, reactivity of the core increases when helium flow fluidises the particle bed, but for core expansions too large, reactivity decreases again. This gives a promise of simple control and inherently safe operation. When the reactor is made cold critical and helium flow increases, the reactivity gain due to core expansion will be compensated by the reactivity loss due to power increase (power reactivity defect). The maximum power density is therefore limited by the maximum reactivity that can be introduced by means of core expansion. When helium flow increases beyond k_{eff} has reached its maximum (see figure 8), reactivity decreases again and power will level off to balance this. As a result, the reactor power depends on the helium flow, and a coolant flow too large or too small will shut down the reactor. Besides this, the reactor power depends on the temperature of the helium that is used as a coolant. Like an "ordinary" helium-cooled graphite-moderated high temperature reactor, an increase of helium temperature reduces reactor power and vice-versa, while on the other hand, an increase of helium temperature reduces the coolant density, which reduces the expanded core height. The latter effect can give either a positive or a negative reactivity introduction depending on the starting point. Clearly, these combined dynamics of fluidisation and neutronics need further investigation.

Thirdly, experiments with a small-scale fluidised bed have shown that the particle density distribution in the cavity is a very complex function of space and time. Although the effects of this on reactivity have to be investigated yet, most of the fluctuations occur with very high frequency for which the zero-power reactivity transfer function has low magnitude. Therefore, these effects are expected to be very weak. Nevertheless they need further investigation

Finally, another important effect to investigate is the possibility of passive decay heat removal after a shut down of the reactor. At this stage it is not sure whether the thermal conduction of the fuel and moderator suffices to keep fuel temperatures below their limit above which failure may occur.

VIII. REFERENCES

1. H. Van Dam, T.H.J.J. van der Hagen, J.E. Hoogenboom, V.A. Khotylev, R.F. Mudde, *Statics and Dynamics of a Fluidized Bed Fission Reactor*, Proc. ICENES'98, Tel Aviv, June 28-July 2, pp 609-616 (1998).
2. Kugeler, K. and Schulten, R., *Hochtemperatur-Reaktor-Technik*, Springer Verlag, Berlin (1989).
3. V.V. Golovko, J.L. Kloosterman, H. van Dam, T.H.J.J. van der Hagen, *Fuel Particle Design for a Fluidized Bed Reactor*, Proc. Jahrestagung Kerntechnik'99, Karlsruhe, May 18-20, 1999.
4. *SCALE-4.3, A Modular Code System for Performing Standardized Computer Analyses for Licensing Evaluation* manual, Oak Ridge National Laboratory, CCC-545.
5. D.R. Vondy, T.B. Fowler, G.W. Cunningham, *BOLD-VENTURE IV, A reactor Analysis Code System, Version IV*, Oak Ridge National Laboratory, NEA CCC-459.
6. J.F. Briesmeister, *MCNP-A General Monte Carlo N-Particle Transport Code, Version 4B*, LA-12625-M, Los Alamos National Laboratory (1997).
7. S. Feher, J.E. Hoogenboom, P.F.A. de Leege and J. Valko, *Monte Carlo Calculation of Dancoff Factors in Irregular Geometries*, Nucl. Sci Eng., **117**, 227-238 (1994).
8. J.L. Kloosterman, *Program VAREX, A Tool for Variational Analysis of Reactivity Effects with XSDRNPM*. Report ECN-I-95-037, Netherlands Energy Research Foundation (ECN), Petten, Netherlands, Oct 1995.
9. W.J.M. de Kruijf, A.J. Janssen, *On the Definition of the Fuel Temperature Coefficient of Reactivity for Pin-Cell Calculations on an Infinite Lattice*, Ann. Nucl. Energy, **20**, № 9, pp. 639-648 (1993).
10. T.H.J.J. van der Hagen, W. Hartevelde, R.F. Mudde and H. van Dam, *Gamma Transmission Measurements on Core Density Fluctuations of a Fluidized Bed Nuclear Reactor*, Proc. IMORN-27, Valencia, Nov 1997, pp 157-164 (1999).